Stable Colloidal Dispersions of a Lipase−Perfluoropolyether Complex in Liquid and Supercritical Carbon Dioxide

Stephanie S. Adkins,[†] Helen R. Hobbs,[‡] Karima Benaissi,[‡] Keith P. Johnston,*[,†] Martyn Poliakoff,[‡] and Neil R. Thomas*[,†]

Department of Chemical Engineering, The University of Texas at Austin, Austin, Texas 78712, and School of Chemistry, University of Nottingham, University Park, Nottingham, NG7 2RD, United Kingdom

Received: August 29, 2007; In Final Form: January 8, 2008

The technique of hydrophobic ion pairing was used to solubilize the lipase from *Candida rugosa* in a fluorinated solvent, perfluoromethylcyclohexane (PFMC), in complex with a perfluoropolyether (PFPE) surfactant, KDP 4606. The enzyme−surfactant complex was determined to have a hydrodynamic diameter of 6.5 nm at atmospheric pressure by dynamic light scattering (DLS), indicating that a single lipase molecule is stabilized by surrounding surfactant molecules. The complex formed a highly stable colloidal dispersion in both liquid and supercritical carbon dioxide at high CO_2 densities (>0.92 and 0.847 g/mL, respectively), with 4% by volume PFMC as a cosolvent, yielding a fluid that was orange, optically translucent, and very nearly transparent. DLS demonstrated aggregation of the enzyme−surfactant complexes in CO_2 at 25 and 40 °C and various pressures (2000−5000 psia) with hydrodynamic diameters ranging from 50 to 200 nm. The mechanism by which the enzyme−surfactant particles aggregate was shown to be via condensation due to very low polydispersities as characterized by the size distribution moments. Interparticle interactions were investigated with respect to density and temperature, and it was shown that on decreasing the CO_2 density, the particle size increased, and the stability against settling decreased. Particle size also decreased as the temperature was increased to 40 °C, at constant CO_2 density. Nanoparticle aggregates of an enzyme−surfactant complex in CO_2, which are nearly optically transparent and stable to settling, are a promising new alternative to previous types of dispersions of proteins in CO_2 that either required water/CO_2 microemulsions or were composed of large particles unstable to settling.

Introduction

Since the first report in the field of biocatalysis by Randolph et al.,[1] over two decades ago, there have been many advances in the field of biocatalysis in supercritical fluids (SCFs), and these have been recently reviewed in detail.[2] Because of the relatively low activity of crude preparations of enzymes in SCFs, many attempts have been made to utilize a stabilized form of an enzyme for use in such solvents. Examples include the use of immobilized enzymes,[3,4] lipid-coated enzymes,[5−8] sol−gels,[9] cross-linked enzyme crystals (CLECs),[10] cross-linked enzyme aggregates (CLEAs),[11,12] the use of reverse micelles or microemulsions,[13,14] and the use of whole cells.[15] More recently, a new approach for the dispersion of enzymes in supercritical carbon dioxide ($scCO_2$) was described.[16] The technique of hydrophobic ion pairing (HIP) previously was used to solubilize proteins in organic solvents by ion pairing between an anionic surfactant such as aerosol OT (AOT) or sodium dodecyl sulfate (SDS), with the cationic residues (lysine, arginine, and histidine) on the surface of the protein.[17−19] In the case of enzymes, an enhanced catalytic activity was demonstrated.[19−23]

Here, the HIP method was adapted by using a CO_2-soluble perfluoropolyether (PFPE) surfactant to modify the surface of the enzyme forming an enzyme−surfactant complex soluble in fluorinated solvents and dispersible in $scCO_2$.[16] Two biomolecules, cytochrome *c* (Cc) and α-chymotrypsin (CMT), were readily ion paired with the fluorinated surfactant KDP 4606 and were shown to form either solutions or dispersions in perfluoromethylcyclohexane (PFMC) and in $scCO_2$, which were optically clear to the naked eye, in all cases. Dynamic light scattering (DLS) measurements were performed on KDP and these complexes in PFMC to determine the aggregate size. The mode diameter of Cc-KDP was revealed to be 21.2 nm (cf. Cc hydrodynamic radius 1.78 nm by NMR[24]), and the mode diameter for CMT-KDP is 11.7 nm (cf. CMT diameter 3.4 nm by X-ray diffraction[25]). Hence, it was suggested that both complexes contain small aggregates of protein molecules surrounded by surfactant molecules. To the best of our knowledge, this is one of only a few reports to determine the diameter of HIP complexes using DLS. Paradkar and Dordick determined the diameter of CMT-AOT HIP complexes in isooctane at 6.8 nm and suggested that this was consistent with a spherical complex of a CMT ion pairing with AOT molecules.[20] Also, more recently, Akbar et al.[26] reported a direct solubilization of enzyme aggregates in nonaqueous media. In particular, subtilisin Carlsberg extracted with AOT into isooctane was shown to have a diameter of 6.1 nm, and on average, there was one protein molecule within the complex. This is in contrast to the larger diameter of 26.1 nm for reverse micelles (average number of protein molecules not determined).[26] It is anticipated that the higher the number of enzyme molecules per complex, the lower the number of active sites that will be available for catalysis. The flux of substrate to and product away from

* Corresponding authors. Fax: (512) 471-7060; e-mail: kpj@che.utexas.edu. (K.P.J.) and neil.thomas@nottingham.ac.uk (N.R.T.).
[†] The University of Texas at Austin.
[‡] University of Nottingham.

10.1021/jp076930n CCC: $40.75
Published on Web 03/26/2008

individual active sites is also likely to be restricted inside the aggregates. Future studies will determine if there is any correlation between surfactant−enzyme aggregate size and catalytic turnover.

Because of the insolubility of crude enzymes and many stabilized forms of enzymes in CO_2, there has been no opportunity for studying the size and aggregation mechanisms of these molecules in this high-pressure solvent. However, recent advances using the HIP methodology to disperse biomolecules in CO_2 using a PFPE surfactant[16] present us with the challenge of investigating these parameters with respect to the dispersed biomolecules under high-pressure CO_2. Small changes in the system temperature and/or pressure can significantly affect the interactions between the solvent molecules and the stabilizing PFPE ligands, which in turn will affect the steric stabilization of colloids,[27] such as these enzyme−surfactant complexes, and can result in aggregation.

Aggregation of colloids in CO_2 has been studied in systems using the techniques of light scattering,[28] turbidimetry,[29−31] optical microscopy,[32,33] X-ray scattering,[34,35] and neutron scattering.[36] In particular, flocculation and attractive interactions have been observed in many types of PFPE-stabilized colloidal systems such as water-in-CO_2 (W/C) emulsions,[32] W/C microemulsions,[36] hydrophilic silica,[37] and gold nanocrystals.[34] For example, Lee et al. investigated a W/C microemulsion stabilized with a PFPE-based surfactant and reported that, even at high CO_2 densities, the interaction strength measured by SANS exceeded the known value for water-in-alkane microemulsions.[36] Indeed, when longer PFPE chains were used, a stronger stabilization was observed, yet the attractive interactions were not entirely overcome,[32] indicating the strength of the attractive droplet interactions in CO_2 even when stabilized by a PFPE surfactant. In addition, the aggregation of PFPE-coated gold nanocrystals in $scCO_2$ was also observed by Saunders et al. using SAXS.[34] Reversible aggregation of the gold nanocrystals, also known as clustering, was observed at all investigated CO_2 densities due to relatively strong interparticle interactions. The attractive interactions between gold clusters, as described by the structure factor $S(q)$, became stronger as the density decreased. Recently, Dickson et al.[28] measured the density dependence of interactions in CO_2 between core−shell particles with silica cores and a porous cross-linked fluoro-silica shell by DLS. The particles with diameters on the order of a few hundred nanometers could be dispersed at 25 °C at the vapor pressure of liquid CO_2, and the aggregate size increased with a decrease in the density of CO_2.

Here, we demonstrate the extraction of lipase from *Candida rugosa* (CRL) into a fluorinated solvent, PFMC, by means of HIP with the anionic PFPE surfactant, KDP 4606. DLS measurements of CRL-KDP dispersions in PFMC at atmospheric pressure were compared with those in high-pressure CO_2, as a function of temperature and pressure, to illustrate marked differences in the sizes of aggregates. Aggregates of the CRL-KDP molecules were greater than 50 nm in size, even at the highest CO_2 densities, where the dispersion appeared nearly transparent to the naked eye. In addition, the stability of the aggregates, based on changes in diameter with time, and the reversibility of aggregation with changes in pressure are reported. The moments of the size distribution were analyzed to determine as to how much of the aggregation is caused by the condensation of protein molecules relative to coagulation. Thus, the mechanism of aggregation of HIP enzyme−surfactant complexes in CO_2 was elucidated.

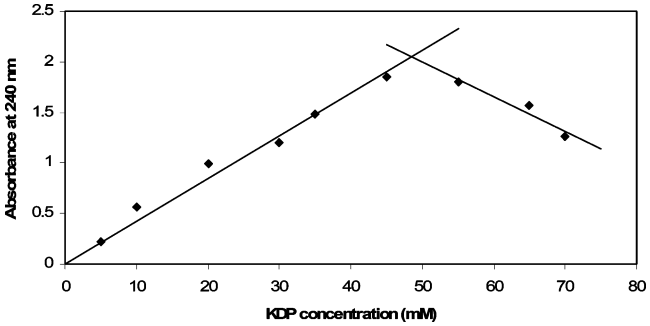

Figure 1. Determination of cmc for KDP 4606 by UV−vis absorption. Intersection of the two lines occurs at 48.4 mM (i.e., 48.4 mM is the cmc for KDP).

Experimental Procedures

Materials. Lipase from *C. rugosa* (CRL, type VII, E.C. 3.1.1.3, 1,140 U/ mg) was purchased from Sigma-Aldrich, and the protein content was determined as 16% w/w by a bicinchoninic acid assay.[24] The perfluoropolyether surfactant KDP 4606 (KDP, MW ∼1400) was kindly donated by DuPont, and PFMC was purchased from Fluorochem. Research grade CO_2 (Matheson) was used in all experiments and was filtered through an oxygen trap prior to introduction to the system.

Determination of Critical Micelle Concentration (cmc) of KDP 4606 in PFMC. The method used to determine the cmc of fluorinated surfactants using UV−vis spectroscopy has been described previously.[38] Solutions of KDP (5−70 mM) in PFMC (1 mL) were stirred with 10 mM sodium phosphate buffer (1 mL, pH 7.0) at 500 rpm for 10 min and then centrifuged at 8000 rpm for 2 min to allow phase separation to occur. The lower fluorous phase was collected, and the concentration of surfactant was analyzed by measuring the absorbance at 240 nm at room temperature using an Agilent 8453 UV spectrophotometer. This measurement was repeated in triplicate. By plotting absorbance against concentration of KDP, it was possible to determine the cmc of KDP in PFMC as 48.4 mM at room temperature, the maximum on the graph shown in Figure 1.

Preparation of CRL-KDP. The preparation of protein−surfactant complexes was previously described.[16] CRL (an off-white powder) dissolved in 10 mM sodium phosphate buffer, pH 7.0 (0.14 mM, 10 mL) was stirred with KDP dissolved in PFMC (23 mM, 5 mL) at 100 rpm for 10 min. The ratio of protein to surfactant was 1:2 w/w, and the KDP concentration was kept below its cmc (49.2 mM). The two resulting phases were left to separate overnight. CRL-KDP in the lower fluorous phase was collected, and the CRL content was analyzed by measuring UV absorbance at 280 nm (CRL-KDP $\epsilon_{280} = 47\,500$ M^{-1} cm^{-1}).[11]

The water content of the CRL-KDP complex in PFMC was analyzed by the Karl Fischer coulometric method and was found to be below the detection level of the instrument (<1 ppm). The known water content of prepared samples could be accurately determined, indicating that neither the PFMC nor the CRL-KDP complex interfered with the measurement.

DLS at Atmospheric Pressure. DLS measurements at atmospheric pressure were carried out on a Zetasizer Nano S at Malvern Instruments. The instrument contained a 4 mW He−Ne laser operating at a wavelength of 633 nm. Each sample was filtered through a 0.2 μm filter (Whatton) prior to measurements, which were made at a detection angle of 173° (i.e., backscatter) and 20 °C. The particle size was taken as the mean value of three measurements. CRL (0.02 mM) dissolved in

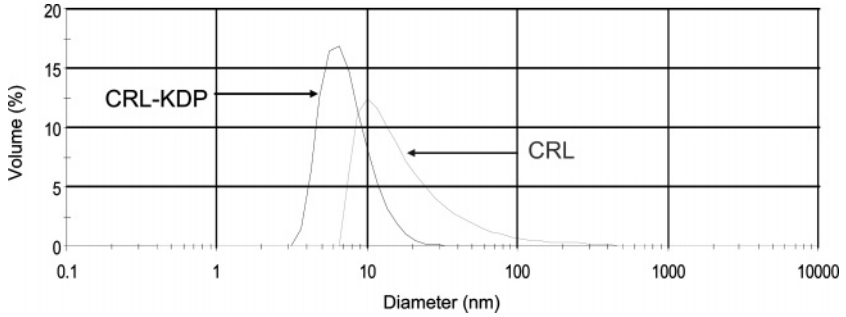

Figure 2. DLS data at atmospheric pressure for CRL in aqueous solution and CRL-KDP in PFMC.

aqueous buffer, CRL-KDP (0.02 mM, protein concentration), and KDP (14 mM) dissolved in PFMC were measured. The data were analyzed using Auto:CONTIN[39] with the following fixed parameters: refractive indexes of 1.333 (water), 1.277 (PFMC), 1.4 (surfactant), and 1.45 (protein) and viscosities (cP) of 1.0019 (water) and 1.561 (PFMC).[40−42]

CRL-KDP Dispersion in CO_2. A protein dispersion was formed by adding CRL-KDP in PFMC (1.7 mM protein concentration, 0.95 mL) and CO_2 (∼20 g) into a high-pressure variable volume view cell (VVVC) described elsewhere.[43] The addition of the CRL-KDP sample to CO_2 as a dispersion in PFMC avoided drying, which is known to cause irreversible aggregation of colloids, as was also demonstrated in a recent study of colloidal interactions between silica particles in CO_2.[28] The amount of PFMC in the system was 4% by volume, and CRL-KDP was 0.42% by weight of the total system. The contents of the high-pressure view cell were continuously mixed with a magnetic Teflon stir bar. The cell was heated to 25 °C, and the pressure was increased to approximately 5000 psia by decreasing the volume of the cell using the hydraulic pump. The pressure was decreased slowly by increasing the cell volume, and visual observations were recorded. The procedure was repeated at 40 °C.

DLS in CO_2. A CRL-KDP dispersion in CO_2 was formed as described previously, in a high-pressure VVVC suitable for carrying out DLS measurements as described elsewhere.[44,45] Briefly, a high-pressure VVVC was connected to a high-pressure homogenizer (Avestin, model C-5), providing recirculation of the cell contents, which was connected to a scattering cell, which in turn was connected back to the VVVC. No filter was used within the system, as the aggregates tended to plug up filters. The system temperature was controlled to ±0.1 °C by immersing the view cell and homogenizer in water baths equipped with temperature controllers (Julabo, Inc). Recirculation lines were maintained at the desired temperature through the use of water-jackets; all other lines were insulated. The scattering cell was insulated with heating tape, and the temperature was controlled to ±0.1 °C by a digital controller (Micromega, model CN76000).

The protein dispersion was formed at 25 °C, and the system was pressurized to 5000 psia. The dispersion was recirculated through the scattering cell for 3−5 min. The pressure drop across the homogenizing valve was 5000 psia. The scattering cell was isolated and equilibrated for ≥2 min to minimize convection currents. DLS scans were taken over 5−10 min, and the measurements were conducted at least 3 times. The coherent light source was a 17 mW He−Ne laser at a wavelength of 633 nm, and the scattered light was collected by a collimator (NSG America, SELFOC microlens, 1.8 mm diameter, 0.25 pitch) coupled to an optical fiber (NSG America, single mode, specified wavelength of 630 nm), and detected by an avalanche photodiode (system designed by Brookhaven Instruments). A digital autocorrelator (Brookhaven Instruments, model BI-9000AT) with 522 real time channels and a non-negative least-squares (NNLS) program was used to analyze the data, and the measured detection angle was 15°. DLS measurements were repeated at various decreasing and increasing pressures. The temperature was increased to 40 °C, and the measurements were repeated in the same way. The measurements were also repeated at 25 °C over 5 days. The polydispersity of each measurement was calculated (SD as a percentage of CRL-KDP mean diameter).

Reversibility Study. CRL-KDP aggregation was examined for reversibility by subjecting the dispersion to large rapid changes in pressure. DLS measurements were conducted at 5000 psia and 25 °C, following ∼3 min shearing by the homogenizer. The system was rapidly depressurized to 1000 psia. After 30 min at this pressure, the system was rapidly pressurized back to 5000 psia and sheared for 2 min before further DLS measurements were taken.

Stability Study. CRL-KDP stability in CO_2 was investigated under the following conditions: 5000 psia, 25 °C; 3350 psia, 25 °C; 5000 psia, 40 °C; and 3325 psia, 40 °C. The dispersion was recirculated for 5 min with the homogenizer, the scattering cell was then isolated, and a series of 10 min DLS scans were conducted over a 90 min period, with no further recirculation. Each time point was defined as the start of each scan (i.e., 0, 10, 20, etc. min). The DLS intensity was normalized by dividing the intensity at each time point by the initial intensity for ease of comparison.

Results

DLS at Atmospheric Pressure. DLS measurements for CRL in aqueous solution and KDP and CRL-KDP in PFMC were conducted on a Malvern Zetasizer Nano and are shown in Figure 2. CRL, a hydrophobic protein, is likely to aggregate and form large particles on dispersion in aqueous medium as shown by a mode diameter of 10.1 nm and high polydispersity. However, on solubilizing CRL in PFMC by means of ion pairing with the highly fluorinated surfactant KDP, the enzyme is stabilized as a single molecule surrounded by surfactants as seen by a mode diameter of 6.5 nm (cf. literature maximum CRL diameter of 5 nm).[46] The measurements were repeated using a BI-ZetaPlus DLS instrument (Brookhaven Instruments), and CRL-KDP was shown to be approximately 6.5 nm, demonstrating excellent reproducibility of results. The CRL-KDP complex in PFMC was transparent and brown.

Dispersion Formation in CO_2. Figure 3 shows a series of photographs of the CRL-KDP dispersion in PFMC/CO_2 at 25 °C in a custom-made VVVC.[43] At higher pressures (>3500 psia), the majority of the CRL-KDP complex was dispersed, giving a characteristic orange translucent state (5050 psia, Figure 3). It is thought that the saturation point of the complex in this particular system was reached due to the observation of a few

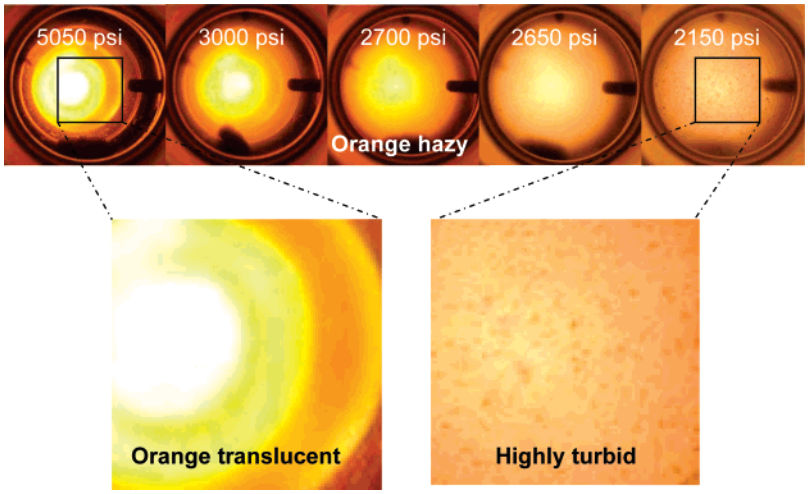

Figure 3. CRL-KDP states in the VVVC at 25 °C at various pressures. At higher pressures, CRL-KDP is almost fully soluble, and the cell is observed to be translucent orange. Decreasing pressure results in a gradual decrease in CRL-KDP solubility indicated by cloudiness or an orange hazy state at around 2700 psi. Below 2650 psi, the CRL-KDP particles begin to precipitate and can be seen to deposit on the cell window, yielding a highly turbid state.

particles on the bottom of the cell that settled. Clearly, it was not possible to determine with the naked eye as to whether the individual protein chains were dissolved at the molecular level, as in the case of PFMC, or if the chains formed some type of dispersed aggregates that scattered light. It would be difficult to predict as to which of these possibilities is more likely from previous studies of related colloids in CO_2. Potential factors that disfavor the dissolution of individual molecules are the relatively high molecular weight of the CRL-KDP complex and the unusually weak solvent strength of CO_2 for stabilizing attractive interactions between droplets in water/CO_2 microemulsions of similar size that are stabilized by PFPE surfactants.[36]

On decreasing the pressure below 3000 psia, aggregates were likely to be present as indicated by an orange hazy state. A further decrease in pressure resulted in significant particle growth, yielding a highly turbid state below 2700 psia with particles depositing on the cell window at a much lower pressure (2150 psia, Figure 3). The aggregation process was demonstrated to be reversible, shown by an increase in dispersibility on increasing the pressure and vice versa.

On an increase of temperature to 40 °C (i.e., supercritical conditions), similar observations were made (see Supporting Information figure). Complete dispersion of small aggregates (no settled particles observed) and an orange translucent state were obtained at higher pressures, suggesting that temperature as well as pressure plays an important role in the morphology of aggregates of CRL-KDP in CO_2. An orange hazy state was observed at 3300 psia, and a highly turbid state was observed at 3050 psia and below, slightly higher in pressure than that for the system at 25 °C.

Following depressurization of the cell, a small volume of PFMC (3.35 mL) was added to resolubilize the remaining CRL-KDP complex. The CRL-KDP protein concentration was determined by UV−vis spectroscopy as 16.5 mg/mL; hence, the total mass recovered was 56 mg, 37 mg less than the starting mass. On dismantling the VVVC, an off-white powder was observed on the back window of the cell. This was shown to be native CRL by its catalytic activity and excellent enantioselectivity for the esterification reaction of *rac*-1-phenylethanol with vinyl acetate (see Supporting Information). Both observations suggest that some of the CRL-KDP underwent a decomplexation process when under CO_2 pressure.

DLS in CO_2. CRL-KDP was dispersed in CO_2 in a high-pressure VVVC suitable for carrying out DLS measurements.[44,45] Similar observations were made at 25 and 40 °C as described previously and can be seen in Table 1 alongside the DLS data for each pressure and temperature. Changes in the CRL-KDP size distribution over a period of days at 25 °C were also investigated.

The autocorrelation function plot for four different CO_2 conditions is displayed in Figure 4. A single-exponential decay was observed, and the NNLS fit to the autocorrelation function is displayed. Similar curves were observed at the other CO_2 conditions investigated (not shown). These results indicate a relatively low polydispersity, and the changes in the diffusion coefficient of the particles are observable with changes in solvent conditions.

The mean diameters of the CRL-KDP particles as a function of CO_2 density were determined from DLS measurements as shown in Figure 5. Interestingly, the mean diameter for CRL-KDP dispersed in CO_2 (Table 1 and Figure 5) is over 10-fold greater than that of CRL-KDP in PFMC (6.5 nm, Figure 2), indicating that the molecules form aggregates under these high-pressure conditions. At both temperatures, decreasing the CO_2 density increases the mean diameter of the CRL-KDP particles. As the solvation strength of CO_2 decreases, the interactions between particles led to the growth of the aggregate size. Surprisingly, during depressurization and pressurization, little hysteresis was observed, indicating that the density-dependent aggregation was highly reversible. Given that these aggregates were shown to be nearly transparent and stable against settling, they may be termed as soluble aggregates.

Figure 6 presents the size distributions for three CO_2 densities that are unimodal with narrow polydispersities ($\leq$2%). These are remarkably low as compared to polydispersities observed for several core−shell silica particle dispersions in CO_2 (10−15%)[28] and for perfluorodecanethiol-stabilized silver nanocrystals synthesized in $scCO_2$ (21−92%).[47] One exception is at 0.985 g/mL (day 5, 25 °C), where the polydispersity was shown to be slightly higher at 10% (Table 1). This may be because at this density, the solution was homogenized for only 2 min as compared to the usual 3 or more minutes.

Reversibility Study. Following rapid depressurization from 5000 to 1000 psia, the system became opaque, and then the protein particles were observed to settle out of solution, creating

TABLE 1: CRL-KDP Dispersion Sizes from DLS[a]

pressure (psia)/temp (°C)	density (g/mL)	appearance	time (days)	mean diameter (nm)	polydispersity [SD/mean] (%)
5000/25	0.985	orange translucent	1	114	2
			3	111	3
			5	96	10
4000/25	0.956	orange translucent	1	120	1
			3	121	2
			5	112	1
3350/25	0.934	orange hazy	1	129	1
			3	133	1
			5	125	1
3000/25	0.920	orange hazy	1	153	1
			3	155	1
			5	159	1
2500/25	0.896	highly turbid	1	191	1
2000/25	0.866	highly turbid	1	N/A	N/A
5000/40	0.933	orange translucent	2	73	5
4600/40	0.920	orange translucent	2	108	4
3975/40	0.896	orange translucent	2	127	6
3325/40	0.865	orange hazy	2	161	2
3000/40	0.847	orange hazy	2	316	1
2500/40	0.812	highly turbid	2	N/A	N/A

[a] Mean diameter and polydispersity (SD as percentage mean diameter) of CRL-KDP complex in CO_2 at various CO_2 densities. Appearance as described in Figure 2, and time is number of days the protein was dispersed in CO_2 when measurement was taken. At lower densities, the count rate considerably increased, indicating multiple scattering and preventing accurate measurements from being taken (N/A).

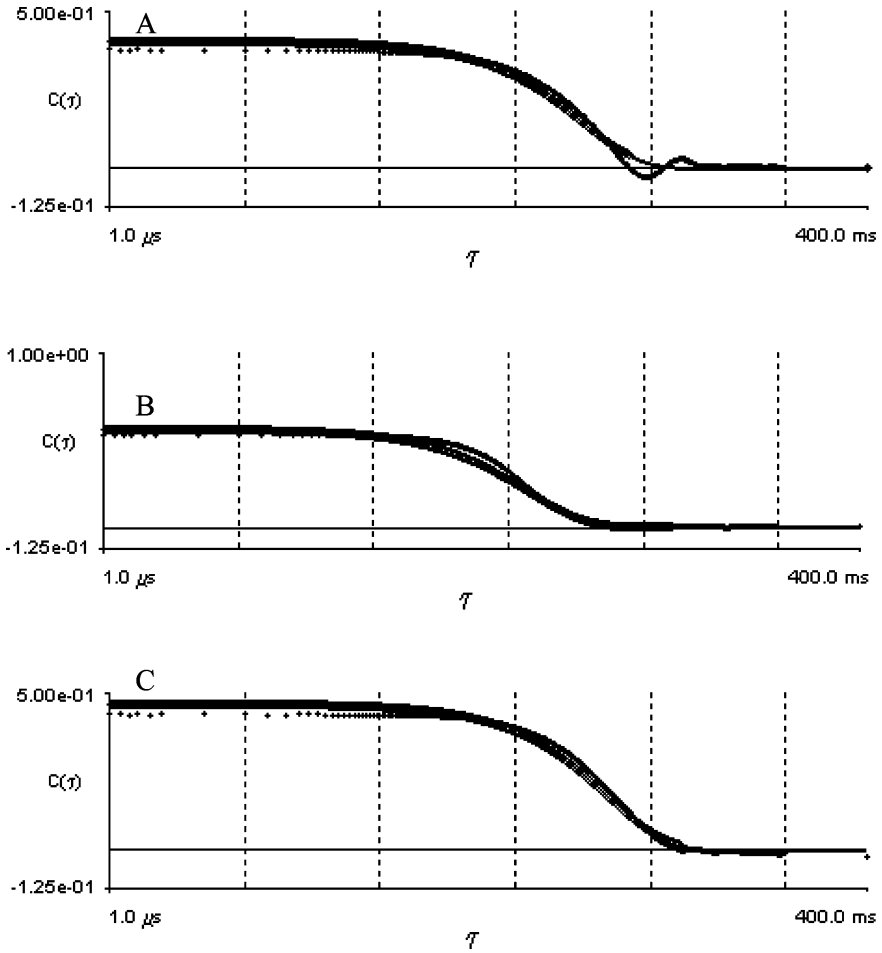

Figure 4. Autocorrelation function graphs of CRL-KDP in CO_2 (dotted lines) and NNLS fit (solid lines): (A) 0.985 g/mL, 25 °C; (B) 0.866 g/mL, 25 °C; and (C) 0.847 g/mL, 40 °C.

a viscous brown coating on the bottom of the cell, which prevented the stir bar from moving. After 30 min, the system was quickly pressurized back to 5000 psia and subjected to shearing for 2 min. The dispersion returned to the orange translucent state. The protein aggregate diameter returned to the original value before depressurization, indicating that aggregation was reversible as the CO_2 density was cycled. The size distribution showed a slight increase in the polydispersity (standard deviation as a percentage of mean diameter), probably due to the short shear time.

Stability Study. Mean diameters of CRL-KDP at four different conditions and various time points are shown in Figure

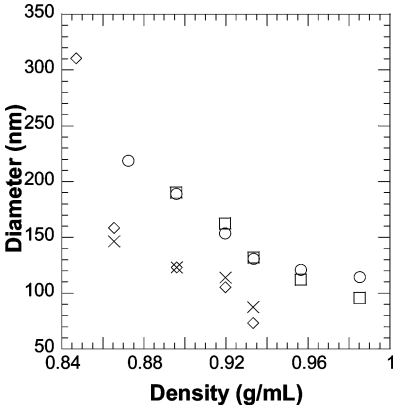

Figure 5. Protein diameter vs CO_2 density on decreasing and increasing pressure. ○: Depressurizing at 25 °C; □: pressurizing at 25 °C; ◇: depressurizing at 40 °C; and ×: pressurizing at 40 °C.

7. Figure 8 shows the normalized intensity for CRL-KDP particles for the highest and lowest CO_2 densities studied. From this, it can be seen that the intensity only changes ca. 20% over the 90 min duration at 0.985 g/mL. However, at 0.865 g/mL, the particle diameter increased from 170 to 230 nm (a 75% increase), followed by a sharp decrease to 115 nm. The behavior of CRL-KDP particles with respect to particle diameter over a period of 90 min suggests further aggregation of the proteins followed by settling of these larger aggregates out of solution at the lowest CO_2 density studied. The higher CO_2 densities did not show this pattern of aggregation and settling and appeared more stable.

Discussion

Comparison of Protein Dispersion in CO_2. The weight fraction of complexes in CO_2 was 1.25%. The weight fraction of protein in CO_2, excluding the weight of PFPE, was 0.42%. This level may be compared to 0.0057% by weight for BSA in W/C microemulsions.[14] Relative to these microemulsions, the HIP strategy of the current paper led to much higher concentrations of protein in CO_2. The ratio of weight of protein to the combined weight of protein and surfactant was 0.42:1.25 (about 1:3), much higher than the typically observed value of 1:10 to 1:1000 for proteins in reverse micelles in an organic solvent[48−50] or the approximate 1:32 ratio of weight of protein to the combined weight of protein and surfactant for subtilisin and Krytox reverse micelles in liquid CO_2 reported by Ghenciu et al.[51] One of the reasons for the higher loadings in CO_2 is that this approach does not depend upon the self-assembly of water and surfactants to form thermodynamically stable microemulsions, with a small water core, and thus a limited payload to dissolve the protein. For reverse micelles or microemulsions, large amounts of surfactant are needed to drive the aggregation of the surfactant to form the micelles. For the complexes, only a small amount of surfactant is required to form an aggregate with weak enough interactions between the aggregates to form a kinetically stable dispersion.

Aggregation of Colloids in CO_2 and Analysis of Growth Mechanisms. Smaller CRL-KDP particles were measured in PFMC; therefore, it can be said that the attraction between protein primary particles is generally much greater in CO_2, even at high densities. In CO_2, it is likely that the PFPE stabilizing ligands were unable to completely screen the Hamaker attraction between the CRL-KDP particles; hence, aggregation occurred (Figure 5), as seen in other PFPE-stabilized systems.[32,34,36]

Condensation and coagulation are the two primary growth mechanisms by which the aggregation of protein colloids may arise. Condensation occurs as individual protein primary particles add to the aggregate, forming a relatively monodisperse size distribution. In contrast, the coagulation of two small aggregates, composed of primary particles, to form a larger aggregate results in a broader size distribution.[52] Size distribution moments, μ_1 and μ_3, are used to determine as to whether aggregation is dominated by condensation or coagulation as shown by the following equations:

$$\mu_1 = \frac{r_3}{r_h} = \left(\frac{3}{\sqrt{\sum r_i^3/N_\infty}}\right)\Big/\left(\frac{N_\infty}{\sum\left(\frac{1}{r_i}\right)}\right) \quad (1)$$

$$\mu_3 = \frac{r_1}{r_3} = \left(\frac{\sum r_i}{N_\infty}\right)\Big/\left(\frac{3}{\sqrt{\sum r_i^3/N_\infty}}\right) \quad (2)$$

where r_1 is the arithmetic mean radius, r_3 is the cube mean radius, r_h is the harmonic mean radius, and N_∞ is the total number of particles. For aggregates formed by condensation, the size distribution moments reflect a monodisperse system, $\mu_1 = \mu_3 = 1$, whereas the size distribution moments for aggregation by coagulation are $\mu_1 > 1.25$ and $\mu_3 < 0.905$.[52]

Table 2 summarizes the calculated size distribution moments for the data presented in Table 1. It is clear that μ_1 and μ_3 approach 1 for all conditions listed, and since the size distribution moments are a ratio of two radii (r_3 and either r_h or r_1) whose values differ by a maximum of 0.02 at 25 °C, it can be said that the calculated moments (μ_1 and μ_3) are very close to unity. This strongly suggests that the enzyme−surfactant complexes aggregate predominantly by a condensation mechanism. This result is also supported by the observation of the very narrow size distributions (see Figure 6).

One reason for the monodisperse distribution of protein aggregates in CO_2 could be a decrease in the kinetics of aggregation as the unimer is depleted. The rate of condensation due to Brownian motion is proportional to the number of aggregates and the number of primary particles present.[53] Therefore, as protein particle aggregates grow from 6.5 to 100 nm, the number of primary particles decreases, hence decreasing the rate of growth by condensation. The rate of condensation also will decrease as the particles grow due to an entropy loss of each individual primary particle as it joins an aggregate. If a balance occurs between this entropy loss and the attractive forces between the aggregates and the primary particles, then the size distribution may be kinetically trapped in a metastable state[28] with a low degree of polydispersity.

Other investigations of the aggregation kinetics of colloids have used techniques such as DLS,[28,54,55] static light scattering (SLS),[56] and TEM.[57] Okuda et al. investigated the time-dependent complex formation of DNA by DLS.[54] They observed that as the particle size increased with short to intermediate incubation time, the polydispersity remained low, but with longer incubation times, this value increased. This was also reported by Ju et al., who studied the aggregation of colloidal silica particles by DLS.[55] In addition, polydispersities of 10−15% were seen for a fluorinated core−shell silica dispersion in liquid CO_2.[28] Furthermore, aerosol studies have shown that a self-preserving condition can exist.[57−60] This occurs after a growth period and is evident by a consistent aggregate size and/or polydispersity over time.

Shah and colleagues investigated perfluorodecanethiol-stabilized silver nanocrystals synthesized in $scCO_2$ with sizes of 20−40 Å depending on the CO_2 density.[47] Calculation of μ_1

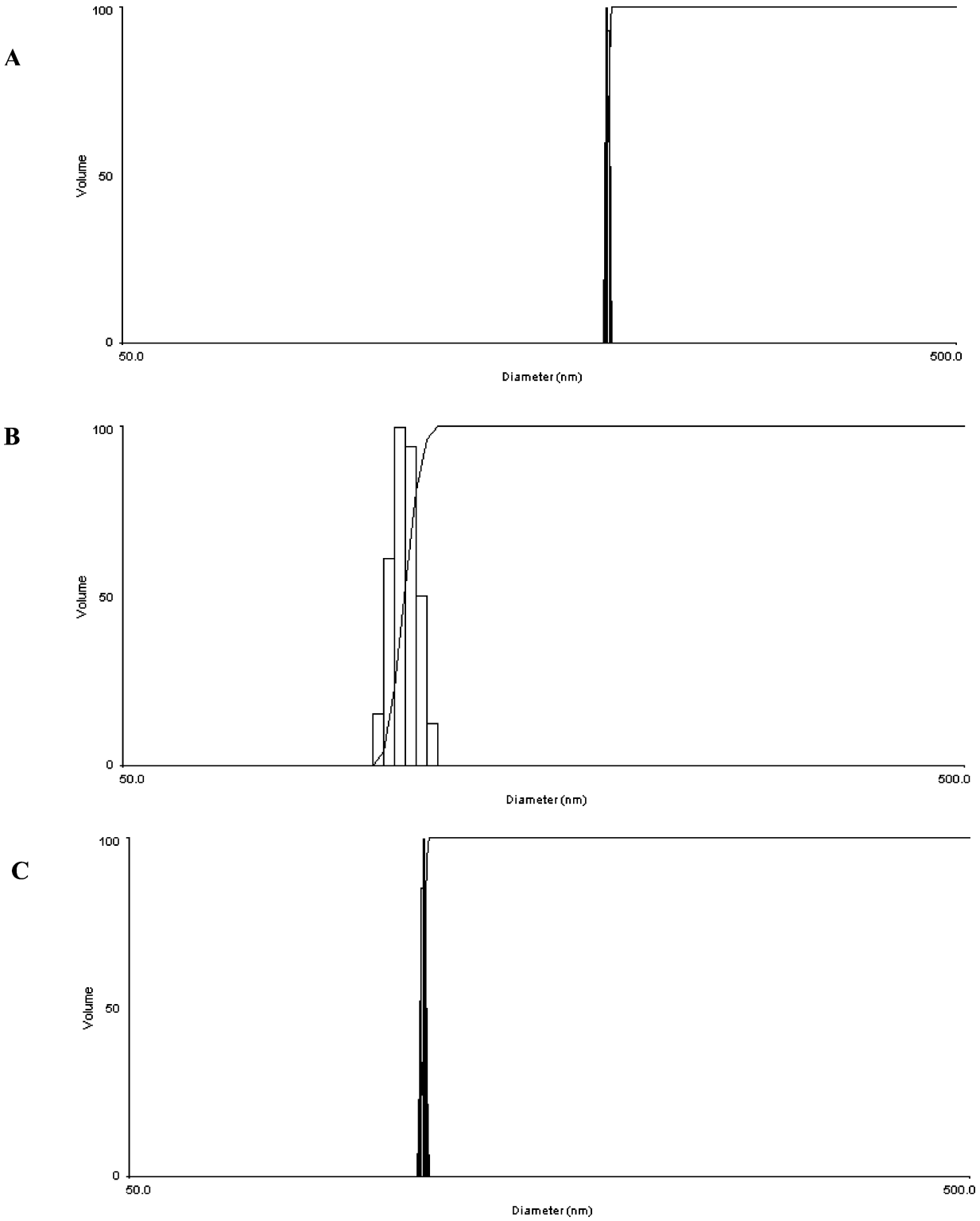

Figure 6. Size distributions of CRL-KDP at various CO_2 densities: (A) 0.866 g/mL, 25 °C; (B) 0.920 g/mL, 40 °C; and (C) 0.985 g/mL, 25 °C.

and μ_3 demonstrated that condensation dominated growth at high CO_2 densities with little coagulation. However, at low CO_2 densities (below 3950 psia and 80 °C), the particles grew by coagulation, and this was due to insufficient solvation of the stabilizing ligands by CO_2. A similar mechanism may be expected to be operative for proteins stabilized by fluorinated surfactants in this study.

The lack of coagulation between protein aggregates may have been facilitated, in part, by void spaces filled with CO_2 between the individual primary particles within the aggregates. The composite Hamaker constant will be lower than that of the primary particles due to the presence of CO_2. Void spaces are not present in the primary particles; thus, condensation of a primary particle with an aggregate will be favored over the coagulation of two aggregates, and this is again reflected in low polydispersities (Figure 6).

Density-Dependent Interparticle Interactions. As the density of CO_2 decreases, the solvation of stabilizing surfactant tails decreases. Neutron scattering,[36] X-ray scattering,[34] light scattering,[61] lattice-fluid theory,[62−64] and Monte Carlo[65] simulations all have suggested the link between tail solvation, CO_2 density, and effect on colloid stability. The aggregation of CRL-KDP

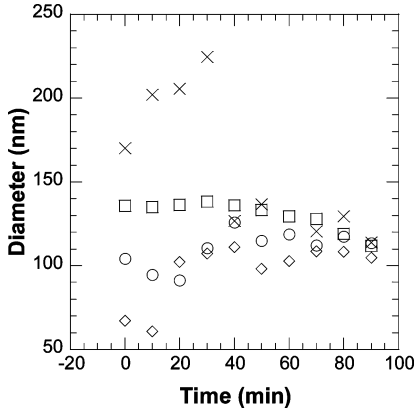

Figure 7. ○: 0.985 g/mL at 25 °C; □: 0.934 g/mL at 25 °C; ◇: 0.933 g/mL at 40 °C; and ×: 0.865 g/mL at 40 °C.

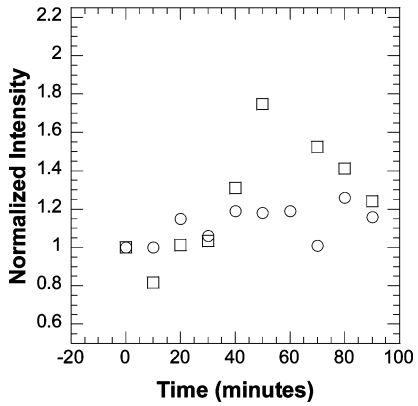

Figure 8. ○: 0.985 g/mL, 25 °C and □: 0.856 g/mL, 40 °C.

TABLE 2: Calculated Size Distribution Moments at Various Conditions

pressure (psi)	temp (°C)	density (g/mL)	μ_1	μ_3
5000	25	0.985	1.000	1.000
4000	25	0.956	1.000	1.000
3350	25	0.934	1.000	1.000
3000	25	0.920	1.000	1.000
2500	25	0.866	1.000	1.000
5000	40	0.933	1.004	0.998
4600	40	0.920	1.003	0.999
3975	40	0.896	1.004	0.998
3325	40	0.865	1.001	1.000
3000	40	0.847	1.000	1.000

particles increases as the density of CO_2 is decreased. CO_2 expands away from the PFPE tails to gain entropy[66] as the density is reduced. The tails become less extended into CO_2, and attractive interparticle tail−tail interactions become stronger, favoring condensation at even lower densities, as shown in Table 1. In addition, the already low Hamaker constant for CO_2 decreases even further as the density is reduced, increasing the difference of the Hamaker constants between CO_2 and PFPE. The result is an increase in the van der Waals force between the CRL-KDP particles. Thus, both a decrease in steric repulsion of the particles and an increase in attractive van der Waals interactions increases the degree of particle aggregation as the density of CO_2 is reduced (Figure 5). The interparticle attractive interactions between the PFPE tails at low densities were reduced at high densities upon repeated cycling, indicating reversibility.

The stability of the dispersed protein aggregates in CO_2 was enhanced by the void spaces between individual protein molecules, which were filled with CO_2. These void spaces weaken the Hamaker attraction between aggregates, as a result of the lower Hamaker constant of CO_2 relative to the protein. This phenomenon was reported by Dickson et al. in their DLS study of core−shell silica particles in liquid CO_2.[28] In addition, the overall density of the aggregates was reduced with the inclusion of voids, which lowers the settling rate. Thus, at high CO_2 densities, the mean aggregate diameter only changed from approximately 105 to 115 nm over 90 min at a density of 0.985 g/mL and 25 °C (Figure 7).

The aggregation and settling of the protein dispersion at a lower CO_2 density (0.856 g/mL, Figure 7) indicates a decrease in colloid stability. The settling rate of a spherical particle, v_s, due to gravity can be calculated from Stoke's Law[53]

$$v_s = [2R_s^2(\rho_s - \rho_f)g]/(9\eta_f) \quad (3)$$

where R_s is the radius of the sphere, η_f is the viscosity of the fluid (CO_2), and ρ_s and ρ_f are the densities of the sphere and fluid, respectively. The radii were obtained from Table 2, the density and viscosity of CO_2 were known, and the density of the protein was estimated at 1.41 g/mL.[67] The resulting settling rates for the protein at CO_2 densities of 0.985 and 0.934 g/mL at 25 °C were calculated as 5.8 and 10.1 μm/min, respectively. At 40 °C, for CO_2 at 0.933 and 0.865 g/mL, the settling rates were 3.3 and 22.0 μm/min, respectively. All of these rates are negligible as compared to the 1.8 cm height of the scattering cell. Thus, observation of particles in the bottom of the cell indicated extensive aggregation to produce much larger particles than those shown in Figure 7 for 0.865 g/mL.

As the CO_2 density is lowered, the calculated settling rates of the aggregates increased due to the larger size of the aggregates (Figures 7 and 8). The enhanced interparticle interactions were caused by the lower Hamaker constant for CO_2 and the decreased solvation of the PFPE, leading to stronger interactions between PFPE ligands. The more rapid settling of the large aggregates, visible as particles settling on the bottom of the cell, also was influenced by the lower solvent viscosity and increased solvent−solute density differences, as seen in eq 3.

Temperature-Dependent Interparticle Interactions. The effect of thermal energy on the solvation properties of CO_2 was studied utilizing Monte Carlo simulations,[68] SANS,[66,69] turbidimetry,[29,30,70] and optical microscopy.[32] Sirard et al. showed that an increase in the temperature, at constant density, increased the extension of end-grafted PDMS polymer brushes in CO_2.[66] This was also seen in the simulation work of Luna Barcena and colleagues, where the mean square end-to-end distance of a Lennard-Jones (L-J) polymer chain increased monotonically as the temperature was raised, at constant density, in a L-J solvent.[68] Melnichenko and co-workers saw a linear increase in the radius of gyration of a polymer in CO_2 as the temperature was raised, at constant density, above the theta condition.[69] A reduction in flocculation, indicating better solvation with higher temperatures, was observed with increasing temperatures for W/C miniemulsions stabilized with poly(1,1-dihydroperfluorooctyl methacrylate)-*b*-poly(ethylene oxide) surfactants[29] and silica with end-grafted poly(1*H*,1*H*-dihydrofluorooctyl methacrylate).[30]

The size of the protein aggregates was smaller at 40 °C relative to 25 °C, as expected due to the increased thermal energy, at constant CO_2 density (Figure 5). In addition, CRL-KDP was dispersible at a lower minimum density at 40 °C than 24 °C, 0.83 and 0.89 g/mL, respectively. The thermodynamic driving force for condensation was reduced by an increase in thermal energy relative to the long-range attractive Hamaker interactions between CRL-KDP particles and the attractive

interparticle tail−tail interactions between PFPE chains.[68] In addition, the stabilizing chains are likely to be more extended as the temperature increases, providing greater repulsion between particles. This effect leads to smaller particles, despite the faster diffusion and collision rates at higher temperatures.

Possible Role of Decomplexation of CRL-KDP in CO_2. It was shown that the CRL-KDP complexes are highly dispersed at CO_2 pressures >3000 psia and 25 or 40 °C. On decreasing pressure, the aggregate size increased (Figure 5) and then decreased upon repressurization. Complete removal of the CO_2 solvent via depressurization could strip some of the PFPE molecules off the protein molecules, hence leaving behind the native CRL powder that was found to be insoluble in PFMC. In addition, decomplexation of the complex also may have contributed to the changes in aggregate size with pressure. KDP is highly soluble in CO_2 in its own right, whereas native CRL is insoluble. On initial pressurization with CO_2 to intermediate pressures, some of the KDP may be stripped off the CRL, resulting in relatively large native CRL aggregates that are not highly dispersible in CO_2. On increasing the pressure further, it is possible that KDP could coat the CRL aggregates more effectively, enabling them to be become smaller and more dispersible in CO_2. The decomplexation may contribute to the high particle diameters (>100 nm) for this sample, in contrast to the smaller diameters (6.5 nm) measured at atmospheric pressure. The observation of native CRL in the cell following complete depressurization supports the concept of decomplexation; however, further investigation is required to characterize the degree of complexation in situ as a function of pressure.

Conclusion

Lipase from *C. rugosa* was modified by ion pairing with an anionic PFPE surfactant, KDP 4606. The concentration of KDP was kept below that of its cmc to ensure that this method was distinguishable from a microemulsion method such as that reported by Panza et al.,[71] whereby an enzyme was solubilized in a fluorous solvent by means of forming fluorinated reverse micelles. The enzyme−surfactant complex was 6.5 nm in diameter by DLS at atmospheric pressure, which strongly suggests that one lipase molecule is surrounded by several surfactant molecules, rendering it soluble in perfluoromethylcyclohexane.

CRL-KDP is readily dispersed in liquid and $scCO_2$ with gentle stirring using PFMC as a cosolvent at densities above 0.92 g/mL (25 °C) and 0.847 g/mL (40 °C) to form a nearly transparent orange dispersion. At these densities and above, the particle sizes were measured by high-pressure DLS and shown to be more than an order of magnitude greater than at atmospheric pressure in PFMC, ranging from 50 to 200 nm, indicating aggregates of the enzyme−surfactant complexes. The growth mechanism for this aggregation was shown to be via condensation as characterized by relatively monodisperse size distribution moments ($\mu_1 \approx \mu_3 \approx 1$). On decreasing the density, the enzyme−surfactant aggregate size increased, similar to the behavior for other colloids including water/CO_2 microemulsions and inorganic particles.[28,36] Upon decreasing density, an increase in attractive interactions between complexes was driven by a gain in the entropy of CO_2 molecules, as they expand away from the complexes, and an increase in the difference in the Hamaker constants for CO_2 and the enzyme complex. The aggregate size was lower at 40 °C than at 25 °C at comparable densities, as the thermal energy becomes stronger relative to the attractive interactions between complexes. Aggregation of CRL-KDP particles in CO_2 at 25 or 40 °C was shown to be reversible with CO_2 pressure. The protein to total solids weight ratio was only 1:3, despite a relatively high solids weight fraction in CO_2 of 1.25%. These reversible and stable concentrated protein nanoaggregates are highly robust and versatile, offering a new route to protein uptake into CO_2 with relatively small surfactant concentrations.

Acknowledgment. This research was supported in part by the STC Program of the National Science Foundation under Agreement CHE987664, the Robert A. Welch Foundation, and the Process Science and Technology Center at the University of Texas. We thank BBSRC, DSM, EPSRC, (EP/C531744/1), and EU (Subclean Probiomat, Grant MEST-CT-2004-007767) for funding. We thank Dr. Michael Kaszuba (Malvern Instruments) for assistance with the atmospheric DLS measurements and Brookhaven Instruments for aid in the design of the custom DLS apparatus.

Supporting Information Available: Digital photographs showing the change in the CRL-KDP dispersion at 40 °C with a decrease in pressure, as well as information regarding the catalytic activity of CRL recovered from the variable volume view cell after depressurization. This information is available free of charge via the Internet at http://pubs.acs.org.

References and Notes

(1) Randolph, T. W.; Blanch, H. W.; Prausnitz, J. M.; Wilke, C. R. *Biotechnol. Lett.* **1985**, *7*, 325.
(2) Hobbs, H. R.; Thomas, N. R. *Chem. Rev.* **2007**, *107*, 2786.
(3) Al-Duri, B.; Goddard, R.; Bosley, J. *J. Mol. Catal. B: Enzym.* **2001**, *11*, 825.
(4) Matsuda, T.; Watanabe, K.; Harada, T.; Nakamura, K.; Arita, Y.; Misumi, Y.; Ichikawa, S.; Ikariya, T. *Chem. Commun. (Cambridge, U.K.)* **2004**, 2286.
(5) Mori, T.; Funasaki, M.; Kobayashi, A.; Okahata, Y. *Chem. Commun. (Cambridge, U.K.)* **2001**, 1832.
(6) Mori, T.; Kobayashi, A.; Okahata, Y. *Chem. Lett.* **1998**, 921.
(7) Mori, T.; Li, M.; Kobayashi, A.; Okahata, Y. *J. Am. Chem. Soc.* **2002**, *124*, 1188.
(8) Mori, T.; Okahata, Y. *Chem. Commun. (Cambridge, U.K.)* **1998**, 2215.
(9) Habulin, M.; Knez, Z. *Acta Chim. Slov.* **2001**, *48*, 521.
(10) Dijkstra, Z. J.; Weyten, H.; Willems, L.; Keurentjes, J. T. F. *J. Mol. Catal. B: Enzym.* **2006**, *39*, 112.
(11) Hobbs, H. R. Biocatalysis in green solvents, Ph.D. Thesis, School of Chemistry, University of Nottingham, 2006.
(12) Matsuda, T.; Tsuji, K.; Kamitanaka, T.; Harada, T.; Nakamura, K.; Ikariya, T. *Chem. Lett.* **2005**, *34*, 1102.
(13) Kane, M. A.; Baker, G. A.; Pandey, S.; Bright, F. V. *Langmuir* **2000**, *16*, 4901.
(14) Johnston, K. P.; Harrison, K. L.; Clarke, M. J.; Howdle, S. M.; Heitz, M. P.; Bright, F. V.; Carlier, C.; Randolph, T. W. *Science (Washington, DC, U.S.)* **1996**, *271*, 624.
(15) Matsuda, T.; Ohashi, Y.; Harada, T.; Yanagihara, R.; Nagasawa, T.; Nakamura, K. *Chem. Commun. (Cambridge, U.K.)* **2001**, 2194.
(16) Hobbs, H. R.; Kirke, H. M.; Poliakoff, M.; Thomas, N. R. *Angew. Chem., Int. Ed.* **2007**, *46*, 7860.
(17) Adjei, A.; Rao, S.; Garren, J.; Menon, G.; Vadnere, M. *Int. J. Pharm.* **1993**, *90*, 141.
(18) Matsuura, J.; Powers, M. E.; Manning, M. C.; Shefter, E. *J. Am. Chem. Soc.* **1993**, *115*, 1261.
(19) Powers, M. E.; Matsuura, J.; Brassell, J.; Manning, M. C.; Shefter, E. *Biopolymers* **1993**, *33*, 927.
(20) Paradkar, V. M.; Dordick, J. S. *J. Am. Chem. Soc.* **1994**, *116*, 5009.
(21) Falk, R.; Randolph, T. W.; Meyer, J. D.; Kelly, R. M.; Manning, M. C. *J. Controlled Release* **1997**, *44*, 77.
(22) Kendrick, B. S.; Meyer, J. D.; Matsuura, J. E.; Carpenter, J. F.; Manning, M. C. *Arch. Biochem. Biophys.* **1997**, *347*, 113.
(23) Bindhu, L. V.; Abraham, T. E. *Biochem. Eng. J.* **2003**, *15*, 47.
(24) Wilkins, D. K.; Grimshaw, S. B.; Receveur, V.; Dobson, C. M.; Jones, J. A.; Smith, L. J. *Biochemistry* **1999**, *38*, 16424.
(25) Krigbaum, W. R.; Godwin, R. W. *Biochemistry* **1968**, *7*, 3126.
(26) Akbar, U.; Aschenbrenner, C. D.; Harper, M. R.; Johnson, H. R.; Dordick, J. S.; Clark, D. S. *Biotechnol. Bioeng.* **2007**, *96*, 1030.

(27) Meredith, J. C.; Johnston, K. P. Theory and Simulation of Colloid and Interface Science in Supercritical Fluids. In *Supercritical Fluids: Fundamentals and Applications*; Kiran, E., Peters, P. D. C., Eds.; Kluwer Academic: Dordrecht, The Netherlands, 2000; p 211.
(28) Dickson, J. L.; Adkins, S. S.; Cao, T.; Webber, S. E.; Johnston, K. P. *Ind. Eng. Chem. Res.* **2006**, *45*, 5603.
(29) Dickson, J. L.; Ortiz-Estrada, C.; Alvarado, J. F. J.; Hwang, H. S.; Sanchez, I. C.; Luna-Barcenas, G.; Lim, K. T.; Johnston, K. P. *J. Colloid Interface Sci.* **2004**, *272*, 444.
(30) Sirard, S. M.; Castellanos, H. J.; Hwang, H. S.; Lim, K.-T.; Johnston, K. P. *Ind. Eng. Chem. Res.* **2004**, *43*, 525.
(31) O'Neill, M. L.; Yates, M. Z.; Harrison, K. L.; Johnston, K. P.; Canelas, D. A.; Betts, D. E.; DeSimone, J. M.; Wilkinson, S. P. *Macromolecules* **1997**, *30*, 5050.
(32) Lee, C. T., Jr.; Psathas, P. A.; Johnston, K. P.; DeGrazia, J.; Randolph, T. W. *Langmuir* **1999**, *15*, 6781.
(33) Sagisaka, M.; Koike, D.; Yoda, S.; Takebayashi, Y.; Furuya, T.; Yoshizawa, A.; Sakai, H.; Abe, M.; Otake, K. *Langmuir* **2007**, *23*, 8784.
(34) Saunders, A. E.; Shah, P. S.; Park, E. J.; Lim, K. T.; Johnston, K. P.; Korgel, B. A. *J. Phys. Chem. B* **2004**, *108*, 15969.
(35) Fulton, J. L.; Pfund, D. M.; McClain, J. B.; Romack, T. J.; Maury, E. E.; Combes, J. R.; Samulski, E. T.; DeSimone, J. M.; Capel, M. *Langmuir* **1995**, *11*, 4241.
(36) Lee, C. T., Jr.; Johnston, K. P.; Dai, H. J.; Cochran, H. D.; Melnichenko, Y. B.; Wignall, G. D. *J. Phys. Chem. B* **2001**, *105*, 3540.
(37) Calvo, L.; Holmes, J. D.; Yates, M. Z.; Johnston, K. P. *J. Supercrit. Fluids* **2000**, *16*, 247.
(38) Mukejere, P.; Gumkowski, M. J.; Chan, C. C.; Sharma, R. *J. Phys. Chem.* **1990**, *94*, 8832.
(39) Provencher, S. W. *J. Chem. Phys.* **1976**, *64*, 2773.
(40) *Dispersion Technology Software (Nanoseries and HPPS*); Malvern Instruments: Malvern, UK, 2002−2003.
(41) Dahl, K.; Biswas, R.; Maroncelli, M. *J. Phys. Chem. B* **2003**, *107*, 7838.
(42) Lide, D. R. *CRC Handbook of Chemistry and Physics: A Ready-Refererence Book of Chemical and Physical Data*, 85th ed.; CRC Press: Boca Raton, FL, 2004.
(43) Licence, P.; Dellar, M. P.; Wilson, R. G. M.; Fields, P. A.; Litchfield, D.; Woods, H. M.; Poliakoff, M.; Howdle, S. M. *Rev. Sci. Instrum.* **2004**, *75*, 3233.
(44) Psathas, P. A.; da Rocha, S. R. P.; Lee, C. T.; Johnston, K. P.; Lim, K. T.; Webber, S. E. *Ind. Eng. Chem. Res.* **2000**, *39*, 2655.
(45) Ryoo, W.; Webber, S. E.; Johnston, K. P. *Ind. Eng. Chem. Res.* **2003**, *42*, 6348.
(46) Grochulski, P.; Li, Y.; Schrag, J. D.; Cygler, M. *Protein Sci.* **1994**, *3*, 82.
(47) Shah, P. S.; Husain, S.; Johnston, K. P.; Korgel, B. A. *J. Phys. Chem. B* **2002**, *106*, 12178.
(48) Goto, M.; Ono, T.; Nakashio, F.; Hatton, T. A. *Biotechnol. Bioeng.* **1997**, *54*, 26.
(49) Leser, M. E.; Luisi, P. L. *Chimia* **1990**, *44*, 270.
(50) Barbaric, S.; Luisi, P. L. *J. Am. Chem. Soc.* **1981**, *103*, 4239.
(51) Ghenciu, E. G.; Russell, A. J.; Beckman, E. J.; Steele, L.; Becker, N. T. *Biotechnol. Bioeng.* **1998**, *58*, 572.
(52) Pich, J.; Friedlander, S. K.; Lai, F. S. *J. Aerosol Sci.* **1970**, *1*, 115.
(53) Shaw, D. J. *Introduction to Colloid and Surface Chemistry*, 4th ed.; Butterworth-Heinemann Ltd.: Boston, 1989.
(54) Okuda, T.; Kidoaki, S.; Ohsaki, M.; Koyama, Y.; Yoshikawa, K.; Niidome, T.; Aoyagi, H. *Org. Biomol. Chem.* **2003**, *1*, 1270.
(55) Ju, R. T. C.; Frank, C. W.; Gast, A. P. *Langmuir* **1992**, *8*, 2165.
(56) Kyriakidis, A. S.; Yiantsios, S. G.; Karabelas, A. J. *J. Colloid Interface Sci.* **1997**, *195*, 299.
(57) Matsoukas, T.; Friedlander, S. K. *J. Colloid Interface Sci.* **1991**, *146*, 495.
(58) Hidy, G. M. *J. Colloid Sci.* **1965**, *20*, 123.
(59) Friedlander, S. K. *Smoke, Dust, and Haze*; John Wiley and Sons: New York, 1977.
(60) Friedlander, S. K.; Wang, C. S. *J. Colloid Interface Sci.* **1966**, *22*, 126.
(61) Yates, M. Z.; O'Neill, M. L.; Johnston, K. P.; Webber, S.; Canelas, D. A.; Betts, D. E.; DeSimone, J. M. *Macromolecules* **1997**, *30*, 5060.
(62) Peck, D. G.; Johnston, K. P. *Macromolecules* **1993**, *26*, 1537.
(63) Meredith, J. C.; Johnston, K. P. *Macromolecules* **1998**, *31*, 5507.
(64) Meredith, J. C.; Johnston, K. P. *Macromolecules* **1998**, *31*, 5518.
(65) Meredith, J. C.; Johnston, K. P. *Langmuir* **1999**, *15*, 8037.
(66) Sirard, S. M.; Gupta, R. R.; Russell, T. P.; Watkins, J. J.; Green, P. F.; Johnston, K. P. *Macromolecules* **2003**, *36*, 3365.
(67) Fischer, H.; Polikarpov, I.; Craievich, A. F. *Protein Sci.* **2004**, *13*, 2825.
(68) Luna-Barcenas, G.; Meredith, J. C.; Sanchez, I. C.; Johnston, K. P.; Gromov, D. G.; de Pablo, J. J. *J. Chem. Phys.* **1997**, *107*, 10782.
(69) Melnichenko, Y. B.; Kiran, E.; Heath, K. D.; Salaniwal, S.; Cochran, H. D.; Stamm, M.; Van Hook, W. A.; Wignall, G. D. *J. Appl. Crystallogr.* **2000**, *33*, 682.
(70) Visintin, P. M.; Carbonell, R. G.; Schauer, C. K.; DeSimone, J. M. *Langmuir* **2005**, *21*, 4816.
(71) Panza, J. L.; Russell, A. J.; Beckmann, E. J. *ACS Symp. Ser.* **2002**, *819*, 64.